Journal of NeuroVirology, 9: 452–464, 2003

ISSN: 1355-0284 print / 1538-2443 online
DOI: 10.1080/13550280390218751

Taylor & Francis
Taylor & Francis Group

Central nervous system correlates of behavioral deficits following simian immunodeficiency virus infection

Michael R Weed,[1] Robert D Hienz,[1] Joseph V Brady,[1] Robert J Adams,[2] Joseph L Mankowski,[2] Janice E Clements,[2] and M Christine Zink[2]

[1]*Department of Psychiatry and Behavioral Sciences, Behavioral Biology Research Center;*
[2]*Department of Comparative Medicine, Johns Hopkins University School of Medicine, Baltimore, Maryland*

Despite the high incidence of cognitive and motor impairment in acquired immunodeficiency syndrome (AIDS) patients, the mechanisms of AIDS-related central nervous system (CNS) pathology are not completely understood. Infection with simian immunodeficiency virus (SIV) in macaques provides an excellent model of AIDS, including human immunodeficiency virus (HIV)-induced CNS pathology and cognitive/behavioral impairment. Co-inoculation with two SIV strains, SIV/17E-Fr and SIV/DeltaB670, accelerates SIV CNS disease, producing SIV encephalitis in over 90% of pig-tailed macaques within 3 months. In the present study, this SIV model was employed to identify cellular and viral correlates of behavioral impairment following SIV infection. Measures of psychomotor speed (simple reaction time), fine motor control (bimanual motor task), and general motor activity (home cage movement) were all adversely affected by SIV disease. Prior to euthanasia, performance was significantly impaired in both a simple reaction time task in 6 of 12 monkeys and a bimanual motor task in 5 of 6 monkeys. All monkeys evaluated (11 of 11) showed significant reductions in spontaneous motor activity. Significant correlations were found between impaired performance on the bimanual motor test and axonal damage (accumulation of β-amyloid precursor protein in the corpus callosum) as well as increased microglial activation and macrophage infiltration (levels of CD68 and Ham56 immunostaining). These results suggest that axonal damage is related to the behavioral impairment induced by infection with SIV. The axonal damage may result from neuroimmune responses, including microglial and macrophage activation. Therefore, axonal damage may be a morphologic manifestation of neuronal dysfunction that underlies development of behavioral impairment in HIV/SIV CNS infection. *Journal of NeuroVirology* (2003) **9,** 452–464.

Keywords: β-amyloid protein precursor; motor activity; reaction time

Introduction

Early in the course of infection, human immunodeficiency virus (HIV) enters the central nervous system (CNS), and although HIV remains in the CNS, HIV does not productively infect neurons (Davis *et al*, 1992; Gendelman *et al*, 1994; Gray *et al*, 1993; Kaul *et al*, 2001). The neurotoxicity resulting from CNS HIV infection is the result of an indirect mechanism, possibly involving toxic viral proteins or inflammatory mediators produced by activated macrophages and microglia (Diesing *et al*, 2002; Gartner, 2000; Lane *et al*, 1996b; Nuovo and Alfieri, 1996; Sharer,

Address correspondence to Michael R Weed, PhD, Johns Hopkins School of Medicine, Department of Psychiatry and Behavioral Sciences, Behavioral Biology Research Center, Johns Hopkins School of Medicine, 5510 Nathan Shock Drive, Baltimore, MD 21224, USA. E-mail: mweed@jhmi.edu

The research reported was conducted with the excellent assistance provided by Rachel Cooper, Deborah Van Kempen, Sandra Sauer, and Chris Pyle in collecting the behavioral data and Jennifer Bennett, Brandon Bullock, Jesse DeWitt, Suzanne Queen, and Jeff Spelman in collecting the viral and cellular data.

This work was supported by grants DA05831 (to MRW), MH61189 and DA12829 (to MCZ), NS35751 (to JEC), and DA12829 (to RDH).

Received 27 September 2002; revised 6 December 2002; accepted 24 February 2003.

1992). Functional effects of HIV infection in the CNS include minor cognitive/motor disorder (MCMD) seen in approximately 5% of early-stage HIV patients, and 25% to 30% of late-stage patients; additionally, 5% to 15% of symptomatic acquired immunodeficiency syndrome (AIDS) patients develop HIV-associated dementia (Bacellar *et al*, 1994; Glass *et al*, 1993; Heaton *et al*, 1994; Price *et al*, 1988; Sacktor and McArthur, 1997). MCMD often involves slowing of reaction time (RT) performance (Arendt *et al*, 1990; Bornstein *et al*, 1993; Dunlop *et al*, 1992; Karlsen *et al*, 1992; Martin *et al*, 1992), and impairment of other aspects of motor control. Importantly, motor control deficits are also predictors of speed of disease progression (Arendt *et al*, 1989, 1992, 1994).

In developed nations, highly active antiretroviral therapy (HAART) has led to a decline in mortality from AIDS and an apparent decline in the prevalence of CNS effects of AIDS (Clifford, 2000; Sacktor *et al*, 2001). HAART has also been reported to be beneficial in cases of HIV-associated dementia and MCMD as well (Chang *et al*, 1999; Clifford, 2000; Gendelman *et al*, 1998; Suarez *et al*, 2001), although as many as 40% of demented patients may not improve with HAART treatment (Dougherty *et al*, 2002). Additionally, treatment failure has become a significant concern with HAART, due to noncompliance, development of resistant strains, intolerable side effects, or other causes (d'Arminio Monforte *et al*, 1998; Ledergerber *et al*, 1999; Wit *et al*, 1999). Moreover, the cost of these treatments reduces their availability for HIV-infected individuals in developing countries. Furthermore, most HIV therapeutics do not readily penetrate the blood-brain barrier, and the long-term effects of reducing peripheral viral loads while sparing virus in the CNS are not well understood. Therefore, understanding the mechanisms of CNS dysfunction induced by HIV remains an important research goal.

Simian immunodeficiency virus (SIV) infection of macaques has proven to be a reliable model of HIV infection in humans, producing a simian AIDS with the advantage of a much shorter disease progression, typically 1 to 2 years. CNS SIV damage also appears mediated by the host's immune response (Berman *et al*, 1999; Desrosiers, 1990; Fox *et al*, 1997; Hirsch and Lifson, 2000; Lane *et al*, 1996a; Rausch *et al*, 1999; Zink *et al*, 1997). SIV disease, like AIDS, involves electrophysiological changes (Berman *et al*, 1999; Pagano *et al*, 1992; Prospero-Garcia *et al*, 1996), slowing of RT performance, and impaired fine motor control; additionally, general motor activity is reliably reduced as SIV disease progresses (Gold *et al*, 1998; Horn *et al*, 1998; Marcario *et al*, 1999a, 1999b; Murray *et al*, 1992; Weed and Gold, 2001). Motor impairment occurs more frequently than cognitive impairment and often precedes cognitive deficits in both SIV and HIV infection (Gold *et al*, 1998; Murray *et al*, 1992; Weed and Gold, 2001).

We have developed an accelerated, consistent model of SIV disease using dual inoculation with a neurovirulent molecularly cloned virus, SIV/17E-Fr, and an immunosuppressive virus swarm, SIV/DeltaB670 (Clements *et al*, 2002; Zink *et al*, 1997, 1999). This dual inoculation produces SIV encephalitis in over 90% of pig-tailed macaques within 3 months, with CNS pathology similar to other SIV strains (Zink *et al*, 1997, 1999). Using this model, we have demonstrated that virus is actively replicating in the brain 10 days post inoculation (p.i.), accompanied by increased expression of macrophage-attracting chemokines, up-regulation of cell adhesion molecules on endothelial cells, and an influx of macrophages to the brain. Further, as with HIV infection, dual-inoculated macaques develop characteristic CNS inflammation that correlates with high brain virus load and high monocyte chemoattractant protein (MCP)-1 levels in the cerebrospinal fluid (CSF) (Brew *et al*, 1997; Ellis *et al*, 1997; McArthur *et al*, 1997; Zink *et al*, 1997, 1999, 2001a). Thus, the accelerated SIV model has the same clinical and pathological features as other SIV/macaque models, but events occur in a more compressed period of time. The compressed time course, along with the high incidence of encephalitis, make the accelerated SIV model useful for studies of the pathogenesis of SIV encephalitis.

The present study used this accelerated SIV model to identify cellular and viral correlates of behavioral impairment. Because motor behaviors are impaired in a high percentage of monkeys infected with SIV, the behavioral measures selected for use in this study concentrated on motor behavior, and included reaction time, general motor activity, and bimanual motor coordination.

Results

Reaction time

Preinfection baseline group mean values for RT performance and all other behavioral variables are presented in Table 1. The effects of SIV disease on reaction-time performance are presented in Figure 1. Figure 1**A** displays group data showing slowing of reaction time without any associated reduction in accuracy (correct trials) or task completion (total trials completed). A repeated-measure analysis of variance (ANOVA) performed on the weekly mean release latency of all monkeys confirmed an overall effect of time following SIV infection on release latency ($F(11, 13) = 3.96,\ P < .01$). Multiple comparisons using the Tukey-Kramer procedure confirmed that the group mean latency in week 13 p.i. differed significantly from that of baseline ($P < .01$). The total number of trials completed during the 1-h sessions varied over time, as confirmed by the repeated measures ANOVA ($F(11, 13) = 3.21,\ P < .01$). However, multiple comparisons using the Tukey-Kramer procedure indicated that no p.i. weekly mean differed from

Table 1 Mean values for cellular, viral, and behavioral measures

CNS measures	*Group mean*	*SEM*	*Units*
β-APP level	305.7	137.8	pixels/field
CD-68	5410.4	1959.2	pixels/field
HAM56 in caudate	1385.1	692.0	pixels/field
Viral antigen (kk41)	1513.6	1461.3	pixels/field
GFAP in gray matter	4.13E+04	1.83E+04	pixels/field
Plasma viral load	1.92E+07	9.28E+06	copy equivalents/mL
CSF viral load	2.99E+06	1.60E+06	copy equivalents/mL
Mean brain viral load	3.86E+06	2.55E+06	copy equivalents/2 μg RNA
Behavioral measures	*Group mean*	*SEM*	
Simple reaction time			
Release latency	439.2	40.0	msec
Percent correct	97.8%	0.6%	
Number of trials	259.1	18.0	
Motor activity	1176.2	133.9	counts/day
Bimanual motor task	35.9	4.2	sec

the baseline condition. Similarly, despite an overall effect indicated by the repeated measures ANOVA ($F(11, 13) = 5.5$, $P < .01$) accuracy at any week following infection with SIV did not differ from baseline. With both the number of trials completed and accuracy, week 2 p.i. differed significantly from weeks later in the second month following infection. These differences most likely produced the significant main effects. Therefore, no significant differences between pre and post infection were apparent for either the number of trials completed or accuracy. False alarm rates did not differ through the experiment (data not shown).

Figure 1**B**, **C** present release latency and total trials measures for individual animals. Release latency increased in three of six monkeys in both the 2- and 3-month groups, as confirmed by the final 1- and 2-week means falling outside the 95% confidence interval around the 2-week preinfection baseline. Total trials completed also differed from baseline in half the animals. Importantly, the animals in which trials completed was reduced were not the same set of animals in which release latency increased. Of the animals with slowed release latency, half performed fewer trials, but half performed the same number of trials. Therefore, there was no obvious relation between reduced task completion and release latency (reaction time).

General motor activity

The baseline group mean value for general activity is presented in Table 1. The effects of SIV disease on general motor activity data are presented in Figure 2 and show a gradual decline in motor activity following infection. A repeated measures ANOVA performed on the weekly mean of 24-h activity counts confirmed an overall effect of time following SIV infection ($F(10, 12) = 8.11$, $P < .01$; Figure 2, *top panel*). Multiple comparisons using the Tukey-Kramer procedure confirmed that the group mean latency in weeks 8, 11, and 12 p.i. differed significantly from that of baseline ($P < .01$). Data from individual animals are presented in the bottom panel in Figure 2 for the weekly mean of weeks 8 and 12 p.i. Weeks 8 and 12 p.i. are presented because they were the week prior to sacrifice for the respective groups. Eight of 10 monkeys showed a decrease during week 8, and 5 of 6 monkeys showed a decrease during week 12 p.i. Additionally, all monkeys showed a decrease in general activity for at least 1 week following infection with SIV with at least one weekly mean falling outside of the baseline's 95% confidence interval. Due to apparatus failure, data for one monkey was lost entirely (364) and another's (D7A) was lost following week 5 p.i.

Bimanual motor task

The baseline group mean value for latency to retrieve all raisins is presented in Table 1. The effects of SIV disease on bimanual motor task performance are presented in Figure 3 and show an impairment in bimanual motor coordination following SIV infection. A repeated-measure ANOVA performed on the weekly mean latency to remove all raisins confirmed an overall effect of time following SIV infection on latency ($F(5, 13) = 2.17$, $P < .05$). Multiple comparisons using the Tukey-Kramer procedure confirmed that the group mean latency in week 13 p.i. infection differed significantly from that of baseline ($P < .05$). On the individual level, latency increased in five of six monkeys, with the means of the last week falling outside the baseline's 95% confidence interval.

Measures of viral and cellular alterations in the CNS

The data for viral and cellular alterations in the CNS measures used in this paper have been published previously (Mankowski *et al*, 2002). Table 1 presents the group mean values for all viral and cellular measures. Figure 4 presents representative photomicrographs of immunostaining for antibodies to CD68 and β-amyloid precusor protein (βAPP).

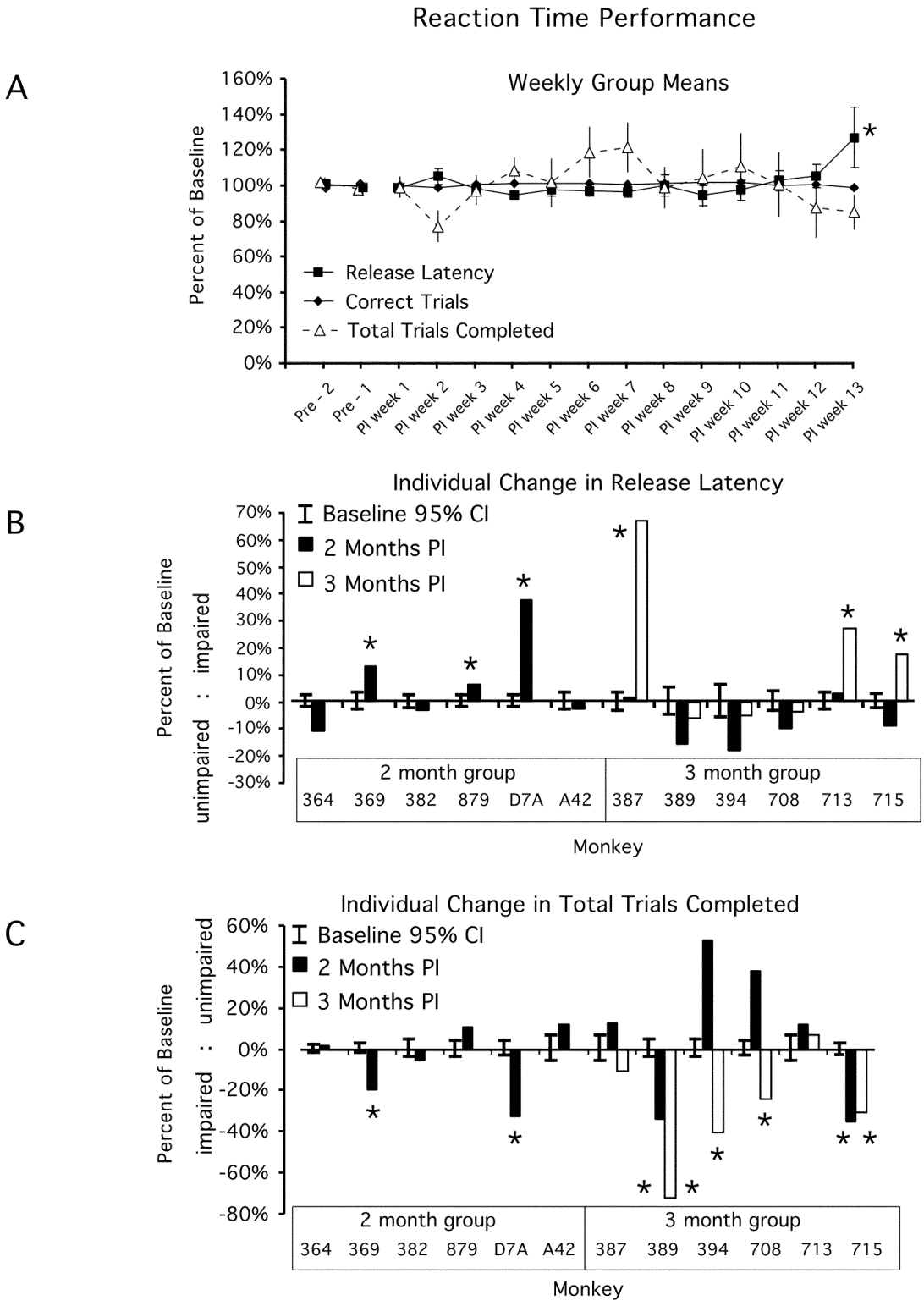

Figure 1 Effects of the accelerated SIV model on reaction time performance. (**A**) Group mean data for release latency, correct trials (accuracy), and total trials completed, with the x-axis representing weeks pre and post inoculation, and the y-axis representing percent of baseline performance. Error bars are the standard error of the mean (SEM). (**B**, **C**) Individual data for release latency and total trials completed, respectively, from the last week prior to euthanasia in both cohorts. The x-axis represents individual monkeys. In both **B** and **C**, the y-axis represents change in the percent of baseline performance. For comparison, data from week 8 for monkeys in the 12-week group is also provided. An asterisk indicates that the point differs significantly from the preinfection baseline ($P < .05$). Note that in **B** impairment from baseline performance produces a positive change, whereas in **C** impairment from baseline produces a negative change. Six of 12 monkeys were significantly slower in performing the RT task following infection relative to their own preinfection baseline.

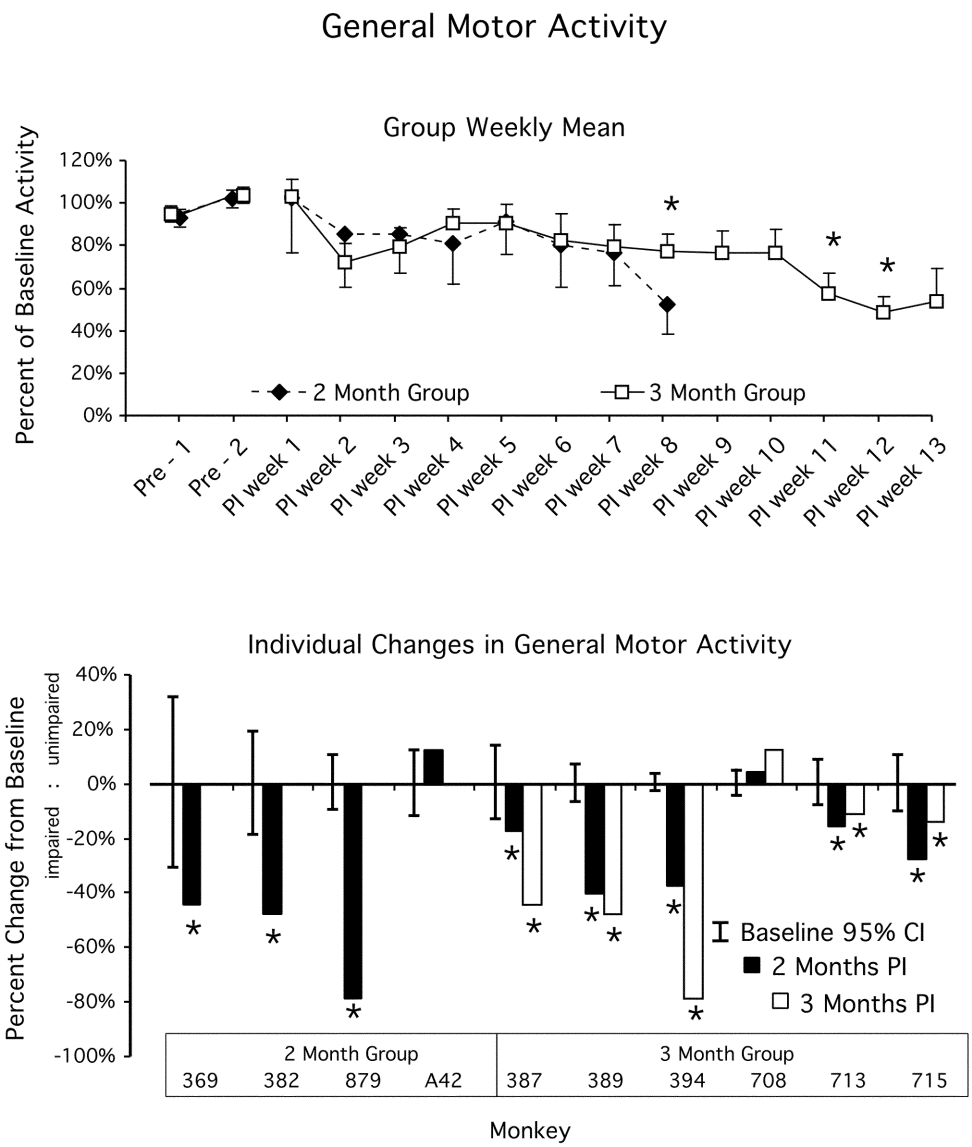

Figure 2 Effects of the accelerated SIV model on general motor activity. Both group mean data and individual animal data showed reduced general activity following infection. The top panel presents weekly group means of 24-h general motor activity, with the x-axis representing weeks pre and post inoculation, and the y-axis representing percent of baseline activity. Error bars are 95% confidence intervals around the baseline mean. The cohorts did not differ in their rate of locomotor decrease. The *bottom panel* presents individual data for general motor activity in the format from Figure 1**B** and **C**. An asterisk indicates that the point differs significantly from the preinfection baseline ($P < .05$).

Comparisons between behavioral and viral/cellular alterations

Table 2 presents r and r^2 values for correlations of the measures of viral and cellular alterations in the CNS with behavioral tests. Figure 5 shows the significant correlations found between performance on the bimanual motor task and markers of axonal damage (β-APP accumulation in the corpus callosum, $r = .99, r^2 = .97, P < .01$), increased microglial activation and macrophage infiltration (levels of CD68 immunostaining, $r = .98, r^2 = .97, P < .01$; levels of Ham56 immunostaining, $r = .91, r^2 = .83, P < .05$) and viral antigen (levels of immunostaining for an antibody to the transmembrane portion of the SIV envelope protein, kk41, $r = .94, r^2 = .89, P < .05$).

When these correlations were tested for their dependence upon outliers, bimanual motor performance correlated significantly with β-APP, CD68, and Ham56 levels with outliers removed; however, the significance of the bimanual motor task versus levels of kk41 was found to be dependent upon one value ($r = .028, r^2 = .08, P > .05$ with monkey 389 removed). Therefore, the relationships between bimanual motor performance, β-APP, CD68, and Ham56 levels were considered significant and robust,

Table 2 Correlations of viral and cellular alterations with behavioral measures

	Behavioral measures					
	Bimanual motor task		*Simple reaction time*		*Motor activity*	
CNS measures	*r*	r^2	*r*	r^2	*r*	r^2
β-APP level	**0.986****	**0.972**	−0.052	0.003	−0.086	0.007
CD-68	**0.984****	**0.967**	−0.045	0.002	−0.107	0.011
HAM56 in caudate	**0.911***	**0.829**	−0.014	0.000	0.216	0.047
Viral antigen (kk41)	0.943	0.889	−0.283	0.080	−0.378	0.143
Plasma viral load	0.855	0.513	−0.279	0.078	−0.321	0.103
CSF viral load	0.777	0.268	0.0178	0.000	−0.317	0.100
Mean brain viral load	0.527	0.278	0.015	0.000	0.129	0.017
GFAP in gray matter	0.574	0.329	−0.013	0.000	0.239	0.057

*indicates $P < .05$, **indicates $P < .01$ (adjusted for multiple comparisons).

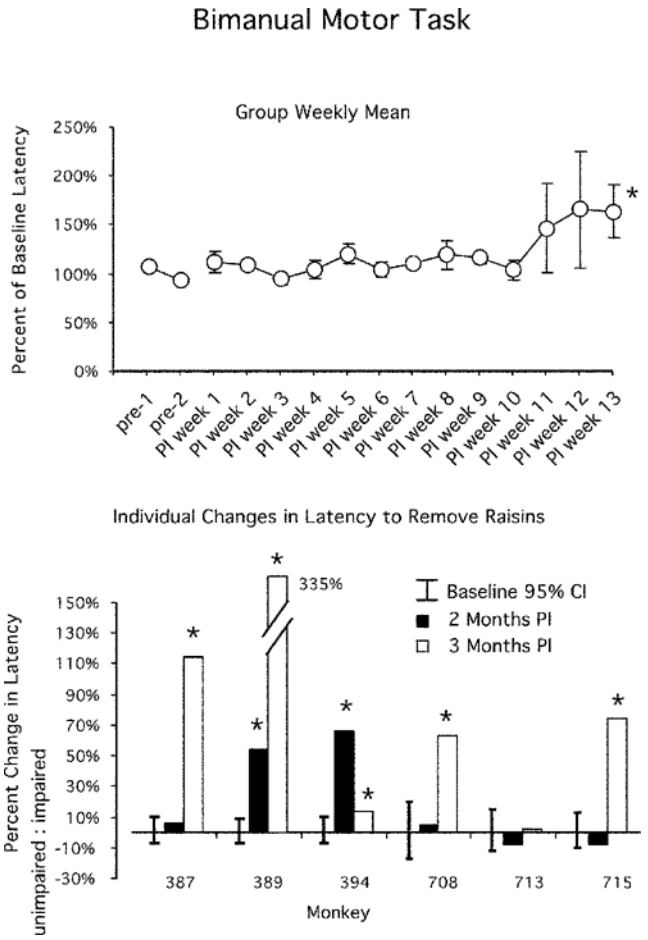

Figure 3 Effects of the rapid SIV model on bimanual motor skill in the 12-week group. Both group mean and individual animals showed impaired ability to perform a task requiring coordination of both hands. *Top:* Weekly group means of latency to remove raisins from a hole-board, with the x-axis representing weeks pre and post inoculation, and the y-axis representing percent of baseline performance. Error bars represent standard error of the mean. *Bottom:* Individual data in the format from Figure 1**B** and **C**. An asterisk indicates that the point differs significantly from the preinfection baseline ($P < .05$). Five of six monkeys were significantly impaired on this task relative to their own preinfection baseline.

but the relationship between kk41 and bimanual motor performance was not.

The results of the assays for viral load and MCP-1 levels in CSF and plasma, β-APP accumulation, CD68 levels, and glial fibrillary acidic protein (GFAP) immunostaining have all been published previously (Mankowski *et al*, 2002).

Discussion

The results of this study show clearly that there is a strong significant correlation between impairment of bimanual motor coordination and the extent of axonal damage detected by measuring immunostaining for β-APP ($r = .99$, $r^2 = .97$, $P < .01$). This finding demonstrates that axonal β-APP accumulation serves as a morphologic marker of neuronal dysfunction associated with behavioral impairment in SIV-infected macaques. Elucidating the mechanisms underlying axonal β-APP accumulation will be essential to identify the molecular basis of neuronal dysfunction and thereby develop new therapeutic approaches to HIV CNS disease.

Previous studies with the SIV/macaque model have demonstrated that dendritic damage occurs following SIV infection (Li *et al*, 1999; Montgomery *et al*, 1999). However, Li *et al* (1999) reported no significant correlation between the extent of dendritic damage and severity of behavioral compromise on a number of behavioral tests, including an RT and fine motor skills task (Li *et al*, 1999). Similarly, neither gross motor activity nor RT performance was significantly correlated with axonal damage, or any other CNS alterations, reported in the present study. It is not surprising that behaviors would be differentially sensitive to differing CNS damage; however, it is not clear why impairments on only the bimanual motor task were correlated with the CNS alterations reported here.

The only measure of neuronal impairment assayed, β-APP accumulation in the corpus callosum, was strongly related to performance on the bimanual motor test. It is quite reasonable to expect that a task

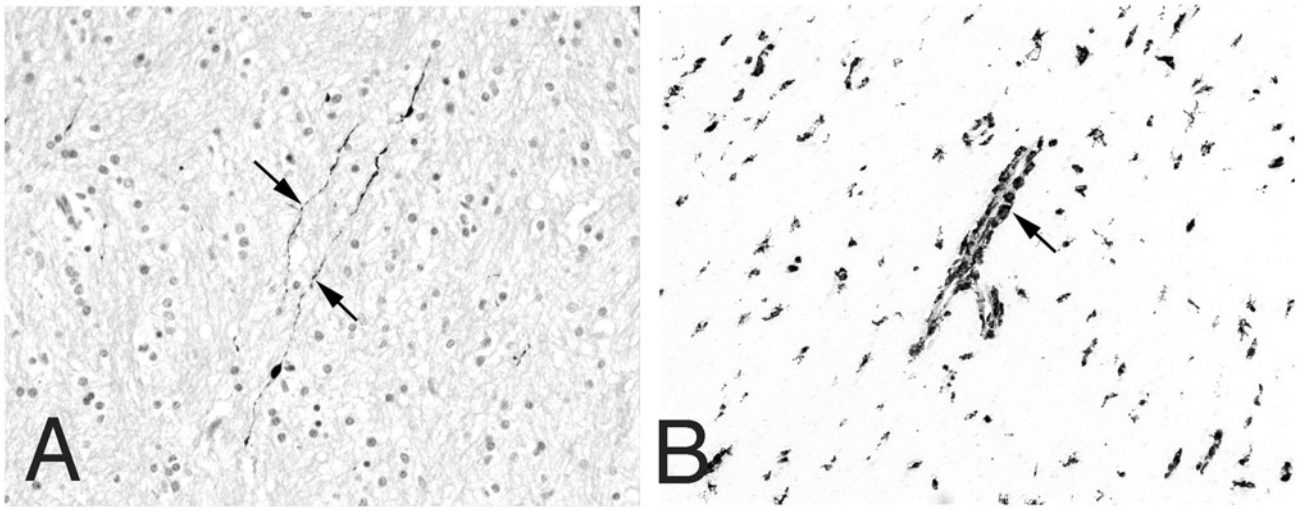

Figure 4 Representative photomicrographs depict immunohistochemical staining for β-APP and CD68 antibodies. (**A**) *Arrows* demonstrate axonal accumulation of β-APP (hematoxylin counterstain). (**B**) CD68-positive perivascular macrophages (*arrow*) and microglia in macaques with SIV encephalitis (no counterstain).

that involves coordinating motor movements from both sides of the body would be especially sensitive to damage in neural pathways connecting both brain hemispheres, such as those in the corpus callosum. Indeed, Mark and Sperry (1968) showed transient impairment in a similar test of bimanual motor coordination in monkeys following a variety of lesions in areas of the corpus callosum and areas with other cerebral cross connections (Mark and Sperry, 1968). It is important to bear in mind that levels of β-APP were increased in a variety of brain areas and that β-APP levels in the corpus callosum were determined to be a convenient metric for comparison between animals due to the sensitivity of our assay in this region. Axonal accumulation of β-APP was also detected diffusely throughout the subcortical white matter in frontal, parietal, and occipital lobes (Mankowski *et al*, 2002), making it difficult to asses whether damage in a particular structure was related to behavioral impairment.

We have previously reported that statistically significant increases in β-APP immunostaining within axons of the corpus callosum were present in 9 of 10 animals examined with SIV encephalitis, whereas only 1 of 14 SIV-infected macaques without encephalitis had elevated β-APP levels over control animal values (Mankowski *et al*, 2002). This association is consistent with the finding in this study that bimanual motor coordination impairment is also correlated with the amounts of CD68 and Ham56 immunostaining, measures of activation of brain macrophages and microglia. These data illustrate that proinflammatory products of activated macrophages and microglia play a role in mediating neuronal dysfunction and corresponding behavioral alterations. Although viral proteins have also been implicated in inducing neuronal damage, this study did not confirm a strong association between the amounts of viral protein in the brain detected by computerized image analysis and the extent of behavioral compromise. Additionally, as in previous reports, levels of astrocyte activation (GFAP staining) and viral load did not correlate with behavioral impairment (Rausch *et al*, 1994).

The results of this study also demonstrate that the accelerated SIV model produces similar behavioral effects to other SIV models (Gold *et al*, 1998; Marcario *et al*, 1999a, 1999b; Murray *et al*, 1992; Weed and Gold, 2001). Specifically, dual inoculation with a neurovirulent molecularly cloned virus, SIV/17E-Fr, and an immunosuppressive virus swarm, SIV/DeltaB670, resulted in reductions in general motor activity, slowed RT, and impairments in bimanual motor coordination.

These results also underscore a feature of the SIV/macaque model that differentiates nonspecific effects of viral infection from the specific effects of SIV infection. Comparison of the behavioral effects during the initial viremia with those later in SIV disease progression provides information as to which effects may be due to a generalized illness and which may be specifically due to progression of SIV disease. Typically, the initial viremia in week 2 post infection affects general motor activity and measures of motivation (e.g., number of trials completed in RT) more strongly than it affects performance of more complex tasks (e.g., bimanual motor skills [BMS], RT latency). Comparison of Figures 1**A**, 2 (*upper panel*), and 3 (*upper panel*) supports this distinction (see also Weed and Gold, 2001). Therefore, a generalized effect of illness, also called 'sickness-behavior,' may be responsible for motivational effects and general motor activity effects, but is not likely to be the cause of the impaired coordination and psychomotor slowing reported.

This study included tests of motor function because of the reliability of motor effects being

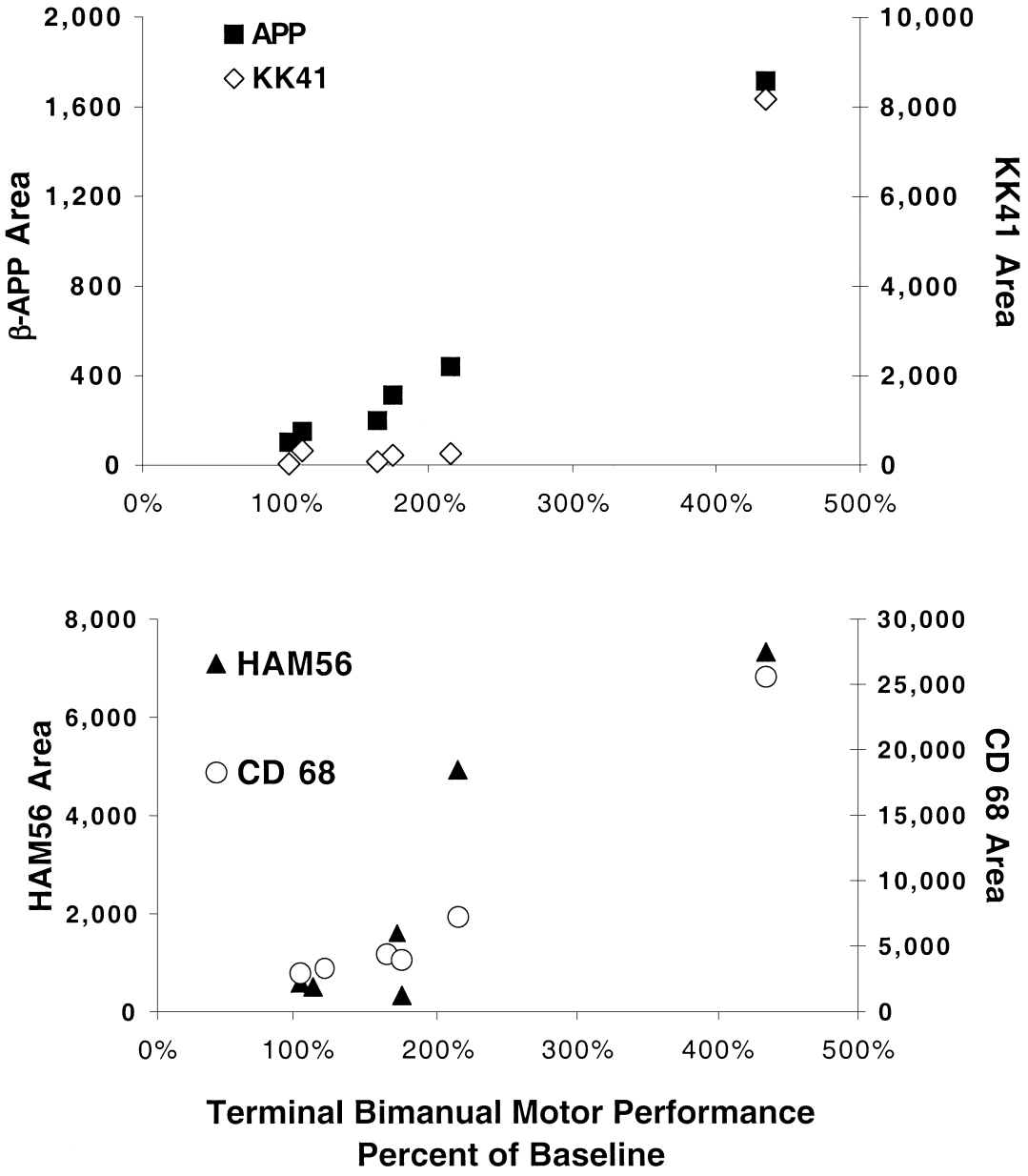

Figure 5 Correlations between performance on the bimanual motor test and markers for β-amyloid precursor protein (β-APP), viral antigen (kk41 immunostaining), and microglial activation and macrophage infiltration (CD68 and Ham56 immunostaining). In both panels, the x-axis represents the average performance for the week prior to sacrifice on the bimanual motor test, relative to preinfection baseline. *Top panel:* The left and right y-axes represent the mean total area of immunostaining (in pixels) for β-APP and kk41, respectively. *Bottom panel:* The left and right y-axes represent the mean total area of immunostaining (in pixels) for CD68 and Ham56, respectively.

produced by SIV disease relative to changes in 'higher' cognitive/behavioral functions, such as learning or memory (Weed and Gold, 2001). The similarity of the behavioral changes and CNS pathology (Mankowski *et al*, 1997; Zink *et al*, 1997, 1998) of the rapid SIV model to other SIV models suggests that the dual-infection model would have similar effects on other behavioral/cognitive domains as well.

Several measures of CNS alterations showed modest but nonsignificant correlations with performance in the bimanual motor test and measures of general motor activity (Table 2). Given the small data set and the alpha adjustment, correlations in this study must be very high to reach statistical significance (for $N = 6$, $r > .907$ and for $N = 12$, $r > .692$ are required to reach significance). Therefore, nonsignificant associations reported here should not be completely discounted and these relationships may be more interesting when investigated with a larger sample size.

The rapid and reproducible onset of CNS disease makes this dual-inoculation model especially useful to study the specific mechanisms by which SIV produces CNS pathology. The development of

behavioral/cognitive changes extends the usefulness of this model and demonstrates its utility in establishing correlation between CNS pathology and behavioral/cognitive impairment. One caveat with the current data set is that monkeys were euthanized at discrete time points, rather than after specific clinical or behavioral end points had been reached by a given individual. The advantage of this euthanasia schedule is that the individual variations in disease progression produces a range of CNS pathology (i.e., they are not all at the end stage of SIV encephalitis) and allows for correlations between animals in different stages of behavioral and pathological decline. However, it is possible that the present study underreports the incidence of behavioral changes produced by the rapid SIV model by terminating the study before some subjects expressed behavioral changes. For instance, all of the monkeys in the 3-month group had slower RT performance at 3-months than at 2-months, although only half of the impairments were statistically significant. It is likely that more animals would show significant behavioral changes if they were allowed to progress to clinical end points. This observation strengthens the importance of the finding that the accelerated SIV model produces reliable behavioral changes.

In summary, the results of this study show clearly that markers of axonal damage (accumulation of β-APP in the corpus callosum) and increased microglial activation and macrophage infiltration (levels of CD68 and Ham56 immunostaining) were significantly correlated with impaired fine motor control. Furthermore, behavioral deficits, including slowed RT, decreased motor activity, and impaired fine motor control, produced by the accelerated SIV model were similar to those seen in other SIV models. These results suggest a relationship between behavioral impairment and axonal damage following infection with SIV. The axonal damage may result from neuroimmune responses, including microglial and macrophage activation. Therefore, axonal damage may be a morphologic manifestation of neuronal dysfunction that underlies development of behavioral impairment in HIV/SIV CNS infection.

Materials and methods

Animals

Two cohorts of six male pig-tailed macaques (3 to 5 kg), all of which were free of Herpesvirus simiae (B-virus), SIV, STLV 1 and 2, and type D retrovirus (SRV-2), were used as subjects. One cohort was euthanized at 2 months and the second at 3 months p.i. Timed euthanasia schedules were used to examine animals at different stages of disease progression; however, if an animal met certain criteria prior to the timed euthanasia (e.g., greater than 15% loss in body weight, failure to eat or drink, clinical symptoms), the animal was euthanized at that point. Three monkeys in the 2-month group (364, 879, A42) reached euthanasia criteria at week 7 p.i. and were euthanized then. The remaining three monkeys were euthanized in week 9 p.i. In the 3-month group, two animals (389 and 394) reached euthanasia criteria and were euthanized in the beginning of week 12 p.i. The remaining monkeys in the 3-month group were euthanized after week 13 p.i. Monkeys were provided with food and water *ad libitum* and housed in a room with a 7AM–9 PM light/dark cycle. Principles of laboratory animal care (*Guide for the Care and Use of Laboratory Animals*, National Academy Press, 1996) were followed, and all protocols were approved by the Institutional Animal Care and Use Committee of The Johns Hopkins University School of Medicine.

Behavioral measures

Reaction time: Response panels were attached daily to each monkey's home cage to conduct the RT task. The panel contained a primate lever, one red and one yellow light-emitting diode used as cue lights, and a cup feeder for delivery of food pellets. The red cue light was used to signal the beginning of each trial, and the yellow cue light was used as the "reaction time" or lever-release signal. The monkeys were trained to press a lever and hold it down in the presence of a flashing red cue light (flashing 5 times per second). A lever press changed the flashing red light to a continuous red light, as long as an animal held the lever down. At intervals ranging from 1.0 to 7.0 s after initiation of the lever holding response, the lever-release signal was presented for 1.5 s on the yellow cue light. Release of the lever within the 1.5 s response window resulted in the delivery of one 190-mg banana-flavored pellet (Bioserv, Frenchtown, NJ), and initiated a 3-s intertrial interval (ITI) during which no stimuli were presented and additional lever responses reinitiated the ITI. Lever releases prior to onset of the release stimulus ("early releases") produced a 4-s timeout without reinforcement. If an animal failed to release the lever, the red cue light was turned off at the end of the 1.5-s response window. Upon lever release, the ITI began without reinforcement. Following the end of the ITI, the flashing red cue light signaled initiation of the next trial in the daily experimental session. To measure the false alarm or "guessing" rate, "catch" trials were randomly interspersed on 20% of the trials. During these catch trials no reaction-time signal occurred. Lever releases during catch trials ("false alarms") resulted in a timeout and initiation of the ITI without reinforcement. Sessions lasted 1 h and were performed at approximately 10 AM each morning, Mondays to Fridays.

In the simple RT procedure, the data collected were (1) percent correct lever releases ("accuracy"); (2) median reaction times; (3) percent false alarms; (4) and total trials completed each session. Baseline performances were defined as stable when (1) the

percentage correct responses were 80% or greater in a session; (2) the false-alarm rates were less than 30%; and (3) there were no systematic changes in these measures across 1 week. Performance during the 2 weeks immediately prior to inoculation was used as each individual animal's preinfection level of performance.

Latency data were analyzed using both individual comparisons to baseline performance (based on 95% confidence intervals around the baseline median) and with repeated-measure analysis of group data (weekly means with the one within-subject factor of time). Accuracy data were also analyzed using both individual comparisons to baseline performance (based on 95% confidence intervals around the baseline mean) and with repeated-measure ANOVA of group data (weekly means with the one within-subject factor of time). Data were transformed using the equation $x = \log 10(x)$, as this increased the homogeneity of the variance between ANOVA cells.

Bimanual motor task: Monkeys in the 3-month group were trained to perform a bimanual motor task. A plastic holeboard with 15 holes (9 mm diameter) spaced 13 mm apart (3 horizontal by 5 vertical array) was filled with raisins and mounted perpendicular to the front of the home cage. Retrieval of the raisins required the monkey to push each raisin with one finger from one side and to pull the raisin from the opposite side with its other hand, requiring bimanual dexterity. Latency to retrieve all 15 raisins was recorded with a stopwatch. To encourage rapid completion of the task, the holeboard was removed promptly upon completion of the task or after a maximum of 3 min. Latency data were analyzed using both individual comparisons to baseline performance (based on 95% confidence intervals around the mean of the last week prior to infection) and with repeated-measure ANOVA of group data (weekly means with the one within factor of time). Data were transformed using the equation $x = \log 10(x)$, as this increased the homogeneity of the variance between ANOVA cells.

General activity: General activity was monitored by attaching a miniaturized activity monitoring device to each monkey via a leather collar (Hienz *et al*, 1992). The monitors recorded minute-by-minute animal movements. Baseline data were recorded prior to SIV infection, and activity was monitored throughout the course of infection. Activity data were reduced to total activity counts per day, after visual inspection of the data showed no advantage to using smaller units of time. Daily mean counts were analyzed using both individual comparisons to baseline performance (based on 95% confidence intervals around the mean of the week prior to infection) and repeated-measure ANOVA of group data (weekly means with the within-subject factor of time). Data were transformed using the equation $x = \log 10(x)$, as this increased the homogeneity of the variance between ANOVA cells.

Measures of viral and cellular alterations in the CNS
The CNS measures were collected as described previously (Mankowski *et al*, 2002; Zink *et al*, 2001b). Brief descriptions of the methods are presented below. Viral load in CSF, plasma, and brain tissue were measured by real time reverse transcriptase–polymerase chain reaction (RT-PCR) as described (Zink *et al*, 1999, 2001b).

Immunohistochemical staining and histopathology: To identify β-APP accumulation in axons, coronal sections of the corpus callosum were immunohistochemically stained with the monoclonal antibody anti-β-APP 695 (Clone LN27; Zymed, South San Francisco, CA). For detection of viral protein, kk41, a monoclonal antibody directed against the SIV transmembrane portion of the SIV envelope, was used (diluted 1:400; AIDS Reagent Program). The antibody Ham56 (diluted 1:50; DAKO, Carpenteria, CA) was used to detect infiltrating macrophages and activated microglia. Primary antibodies against the following antigens were also used to assess CNS cellular alterations: CD68, a marker of microglial activation and macrophage infiltration (KP-1, diluted 1:2,000; DAKO), and GFAP for evaluation of astrocyte activation (diluted 1:4,000; DAKO). All brain tissue sections were stained by an automated immunostainer (Optimax Plus, BioGenex, San Ramon, CA) for uniformity. Streck-fixed, paraffin-embedded brain tissue sections were deparaffinized, rehydrated, and then postfixed in Streck tissue fixative (Streck Laboratories, Omaha, NE) for 20 min. After rinsing in water, tissues were heated in a microwave in sodium citrate buffer (0.01 M, pH 6.0) for 8 min to retrieve antigen. Endogenous peroxidase was quenched with 3% H_2O_2 for 10 min and then sections were blocked with buffered casein for 5 min. Primary antibody was applied to tissue sections for 60 min at room temperature, the tissues were washed in buffer, and then secondary biotinylated multilink antibody (Biogenex, San Ramon, CA) was added for 20 min. After washing, streptavidin–horseradish peroxidase was applied for 20 min, followed by diaminobenzidene tetrahydrochloride in buffer containing H_2O_2 for 10 min. Sections were then washed, dehydrated, and mounted.

Quantitative image analysis: For each animal, 20 adjacent fields in the corpus callosum from sections immunostained for β-APP were captured at 200× magnification (an area of 2.8 mm^2) using a Sensys 2 digital camera (Photometrics, Tucson, AZ), then analyzed by IP Lab imaging software (Scanalytics, Vienna, VA). Similarly, 20 200× power fields were captured in subcortical white matter subjacent to cingulate gyrus for measurement of viral protein, macrophage/microglial activation. GFAP

immunostaining was measured in cortical gray matter of the cingulate gyrus on the same tissue section. Viral load in brain tissues was measured in the parietal cortex, basal ganglia, thalamus, and cerebellum, and the mean of these areas is reported as mean brain viral load. Images were binarized and the total area occupied by immunopositive pixels calculated to measure the total area of immunostaining.

Comparisons between behavioral and viral/cellular alterations: The average behavioral performances from the week prior to sacrifice were compared to measures of viral and cellular alterations using a simple correlation. Results are presented in terms of the associated r, r^2, and P values. Significance levels were adjusted for the number of comparisons for each behavioral variable. For each significant correlation, the dependence upon individual data points was tested by recalculation of the correlation following removal of visible outliers. Correlations found to be dependent on outliers were considered to be not statistically significant.

References

Arendt G, Hefter H, Buescher L, Hilperath F, Elsing C, Freund HJ (1992). Improvement of motor performance of HIV-positive patients under AZT therapy. *Neurology* **42:** 891–896.

Arendt G, Hefter H, Elsing C, Neuen-Jakob E, Strohmeyer G, Freund HJ (1989). New electrophysiological findings on the incidence of brain involvement in clinically and neurologically asymptomatic HIV infections]. *EEG EMG Z Elektroenzephalogr Elektromyogr Verwandte Geb* **20:** 280–287.

Arendt G, Hefter H, Elsing C, Strohmeyer G, Freund HJ (1990). Motor dysfunction in HIV-infected patients without clinically detectable central-nervous deficit. *J Neurol* **237:** 362–368.

Arendt G, Hefter H, Hilperath F, von Giesen HJ, Strohmeyer G, Freund HJ (1994). Motor analysis predicts progression in HIV-associated brain disease. *J Neurol Sci* **123:** 180–185.

Bacellar H, Munoz A, Miller EN, Cohen BA, Besley D, Selnes OA, Becker JT, McArthur JC (1994). Temporal trends in the incidence of HIV-1-related neurologic diseases: Multicenter AIDS Cohort Study, 1985–1992. *Neurology* **44:** 1892–1900.

Berman NE, Marcario JK, Yong C, Raghavan R, Raymond LA, Joag SV, Narayan O, Cheney PD (1999). Microglial activation and neurological symptoms in the SIV model of NeuroAIDS: association of MHC-II and MMP-9 expression with behavioral deficits and evoked potential changes. *Neurobiol Dis* **6:** 486–498.

Bornstein RA, Nasrallah HA, Para MF, Whitacre CC, Rosenberger P, Fass RJ (1993). Neuropsychological performance in symptomatic and asymptomatic HIV infection [see comments]. *AIDS* **7:** 519–524.

Brew BJ, Pemberton L, Cunningham P, Law MG (1997). Levels of human immunodeficiency virus type 1 RNA in cerebrospinal fluid correlate with AIDS dementia stage. *J Infect Dis* **175:** 963–966.

Chang L, Ernst T, Leonido-Yee M, Witt M, Speck O, Walot I, Miller EN (1999). Highly active antiretroviral therapy reverses brain metabolite abnormalities in mild HIV dementia [In Process Citation]. *Neurology* **53:** 782–789.

Clements JE, Babas T, Mankowski JL, Suryanarayana K, Piatak Jr M, Tarwater PM, Lifson JD, Zink MC (2002). The central nervous system as a reservoir for simian immunodeficiency virus (SIV): steady-state levels of SIV DNA in brain from acute through asymptomatic infection. *J Infect Dis* **186:** 905–913.

Clifford DB (2000). Human immunodeficiency virus-associated dementia. *Arch Neurol* **57:** 321–324.

d'Arminio Monforte A, Testa L, Adorni F, Chiesa E, Bini T, Moscatelli GC, Abeli C, Rusconi S, Sollima S, Balotta C, Musicco M, Galli M, Moroni M (1998). Clinical outcome and predictive factors of failure of highly active antiretroviral therapy in antiretroviral-experienced patients in advanced stages of HIV-1 infection. *AIDS* **12:** 1631–1637.

Davis LE, Hjelle BL, Miller VE, Palmer DL, Llewellyn AL, Merlin TL, Young SA, Mills RG, Wachsman W, Wiley CA (1992). Early viral brain invasion in iatrogenic human immunodeficiency virus infection. *Neurology* **42:** 1736–1739.

Desrosiers RC (1990). The simian immunodeficiency viruses. *Annu Rev Immunol* **8:** 557–578.

Diesing TS, Swindells S, Gelbard H, Gendelman HE (2002). HIV-1-associated dementia: a basic science and clinical perspective. *AIDS Read* **12:** 358–368.

Dougherty RH, Skolasky RL Jr, McArthur JC (2002). Progression of HIV-associated dementia treated with HAART. *AIDS Read* **12:** 69–74.

Dunlop O, Bjorklund RA, Abdelnoor M, Myrvang B. (1992). Five different tests of reaction time evaluated in HIV seropositive men. *Acta Neurol Scand* **86:** 260–266.

Ellis RJ, Ksia K, Spector SA, Nelson JA, Heaton RK, Wallace MR, Abramson I, Atkinson JH, Grant I, McCutchan JA, Group HNRC (1997). Cerebrospinal fluid human immunodeficiency virus type 1 RNA levels are elevated in neurocognitively impaired individuals with acquired immunodeficiency syndrome. *Ann Neurol* **42:** 679–688.

Fox HS, Gold LH, Henriksen SJ, Bloom FE (1997). Simian immunodeficiency virus: a model for neuroAIDS. *Neurobiol Dis* **4:** 265–274.

Gartner S (2000). HIV infection and dementia. *Science* **287:** 602–604.

Gendelman HE, Lipton SA, Tardieu M, Bukrinsky MI, Nottet HS (1994). The neuropathogenesis of HIV-1 infection [see comments]. *J Leukoc Biol* **56:** 389–398.

Gendelman HE, Zheng J, Coulter CL, Ghorpade A, Che M, Thylin M, Rubocki R, Persidsky Y, Hahn F, Reinhard J Jr, Swindells S (1998). Suppression of inflammatory neurotoxins by highly active antiretroviral therapy in human immunodeficiency virus-associated dementia. *J Infect Dis* **178:** 1000–1007.

Glass JD, Wesselingh SL, Selnes OA, McArthur JC (1993). Clinical-neuropathologic correlation in HIV-associated dementia [see comments]. *Neurology* **43:** 2230–2237.

Gold LH, Fox HS, Henriksen SJ, Buchmeier MJ, Weed MR, Taffe MA, Huitron-Resendiz S, Horn TF, Bloom FE (1998). Longitudinal analysis of behavioral,

neurophysiological, viral and immunological effects of SIV infection in rhesus monkeys. *J Med Primatol* **27:** 104–112.

Gray F, Hurtrel M, Hurtrel B. (1993). Early central nervous system changes in human immunodeficiency virus (HIV)-infection. *Neuropathol Appl Neurobiol* **19:** 3–9.

Heaton RK, Velin RA, McCutchan JA, Gulevich SJ, Atkinson JH, Wallace MR, Godfrey HP, Kirson DA, Grant I (1994). Neuropsychological impairment in human immunodeficiency virus infection: implications for employment. HNRC Group. HIV Neurobehavioral Research Center [see comments]. *Psychosom Med* **56:** 8–17.

Hienz RD, Turkkan JS, Spear DJ, Sannerud CA, Kaminski BJ, Allen RP (1992). General activity in baboons measured with a computerized, lightweight piezoelectric motion sensor: effects of drugs. *Pharmacol Biochem Behav* **42:** 497–507.

Hirsch VM, Lifson JD (2000). Simian immunodeficiency virus infection of monkeys as a model system for the study of AIDS pathogenesis, treatment, and prevention. *Adv Pharmacol* **49:** 437–477.

Horn TF, Huitron-Resendiz S, Weed MR, Henriksen SJ, Fox HS (1998). Early physiological abnormalities after simian immunodeficiency virus infection. *Proc Natl Acad Sci U S A* **95:** 15072–15077.

Karlsen NR, Reinvang I, Froland SS (1992). Slowed reaction time in asymptomatic HIV-positive patients. *Acta Neurol Scand* **86:** 242–246.

Kaul M, Garden GA, Lipton SA (2001). Pathways to neuronal injury and apoptosis in HIV-associated dementia. *Nature* **410:** 988–994.

Lane JH, Sasseville VG, Smith MO, Vogel P, Pauley DR, Heyes MP, Lackner AA (1996a). Neuroinvasion by simian immunodeficiency virus coincides with increased numbers of perivascular macrophages/microglia and intrathecal immune activation. *J NeuroVirol* **2:** 423–432.

Lane TE, Buchmeier MJ, Watry DD, Fox HS (1996b). Expression of inflammatory cytokines and inducible nitric oxide synthase in brains of SIV-infected rhesus monkeys: applications to HIV-induced central nervous system disease. *Mol Med* **2:** 27–37.

Ledergerber B, Egger M, Opravil M, Telenti A, Hirschel B, Battegay M, Vernazza P, Sudre P, Flepp M, Furrer H, Francioli P, Weber R (1999). Clinical progression and virological failure on highly active antiretroviral therapy in HIV-1 patients: a prospective cohort study. Swiss HIV Cohort Study. *Lancet* **353:** 863–868.

Li Q, Eiden LE, Cavert W, Reinhart TA, Rausch DM, Murray EA, Weihe E, Haase AT (1999). Increased expression of nitric oxide synthase and dendritic injury in simian immunodeficiency virus encephalitis. *J Hum Virol* **2:** 139–145.

Mankowski JL, Flaherty MT, Spelman JP, Hauer DA, Didier PJ, Amedee AM, Murphey-Corb M, Kirstein LM, Munoz A, Clements JE, Zink MC (1997). Pathogenesis of simian immunodeficiency virus encephalitis: viral determinants of neurovirulence. *J Virol* **71:** 6055–6060.

Mankowski JL, Queen SE, Tarwater PM, Fox KJ, Perry VH (2002). Accumulation of beta-amyloid precursor protein in axons correlates with CNS expression of SIV gp41. *J Neuropathol Exp Neurol* **61:** 85–90.

Marcario JK, Raymond LA, McKiernan BJ, Foresman LL, Joag SV, Raghavan R, Narayan O, Cheney PD (1999a). Motor skill impairment in SIV-infected rhesus macaques with rapidly and slowly progressing disease. *J Med Primatol* **28:** 105–117.

Marcario JK, Raymond LA, McKiernan BJ, Foresman LL, Joag SV, Raghavan R, Narayan O, Hershberger S, Cheney PD (1999b). Simple and choice reaction time performance in SIV-infected rhesus macaques. *AIDS Res Hum Retroviruses* **15:** 571–583.

Mark RF, Sperry RW (1968). Bimanual Coordination in Monkeys. *Exp Neurol* **21:** 92–104.

Martin A, Heyes MP, Salazar AM, Kampen DL, Williams J, Law WA, Coats ME, Markey SP (1992). Progressive slowing of reaction time and increasing cerebrospinal fluid concentrations of quinolinic acid in HIV-infected individuals. *J Neuropsychiatry Clin Neurosci* **4:** 270–279.

McArthur JC, McClernon DR, Cronin MF, Nance-Sproson TE, Saah AJ, St. Clair M, Lanier ER (1997). Relationship between human immunodeficiency virus-associated dementia and viral load in cerebrospinal fluid and brain. *Ann Neurol* **42:** 689–698.

Montgomery MM, Dean AF, Taffs F, Stott EJ, Lantos PL, Luthert PJ (1999). Progressive dendritic pathology in cynomolgus macaques infected with simian immunodeficiency virus. *Neuropathol Appl Neurobiol* **25:** 11–19.

Murray EA, Rausch DM, Lendvay J, Sharer LR, Eiden LE (1992). Cognitive and motor impairments associated with SIV infection in rhesus monkeys. *Science* **255:** 1246–1249.

Nuovo GJ, Alfieri ML (1996). AIDS dementia is associated with massive, activated HIV-1 infection and concomitant expression of several cytokines. *Mol Med* **2:** 358–366.

Pagano MA, Cahn PE, Garau ML, Mangone CA, Figini HA, Yorio AA, Dellepiane MC, Amores MG, Perez HM, Casiro AD (1992). Brain-stem auditory evoked potentials in human immunodeficiency virus-seropositive patients with and without acquired immunodeficiency syndrome. *Arch Neurol* **49:** 166–169.

Price RW, Brew B, Sidtis J, Rosenblum M, Scheck AC, Cleary P (1988). The brain in AIDS: central nervous system HIV-1 infection and AIDS dementia complex. *Science* **239:** 586–592.

Prospero-Garcia O, Gold LH, Fox HS, Polis I, Koob GF, Bloom FE, Henriksen SJ (1996). Microglia-passaged simian immunodeficiency virus induces neurophysiological abnormalities in monkeys. *Proc Natl Acad Sci U S A* **93:** 14158–14163.

Rausch DM, Heyes MP, Murray EA, Lendvay J, Sharer LR, Ward JM, Rehm S, Nohr D, Weihe E, Eiden LE (1994). Cytopathologic and neurochemical correlates of progression to motor/cognitive impairment in SIV-infected rhesus monkeys. *J Neuropathol Exp Neurol* **53:** 165–175.

Rausch DM, Murray EA, Eiden LE (1999). The SIV-infected rhesus monkey model for HIV-associated dementia and implications for neurological diseases. *J Leukoc Biol* **65:** 466–474.

Sacktor N, Lyles RH, Skolasky R, Kleeberger C, Selnes OA, Miller EN, Becker JT, Cohen B, McArthur JC (2001). HIV-associated neurologic disease incidence changes: Multicenter AIDS Cohort Study, 1990–1998. *Neurology* **56:** 257–260.

Sacktor N, McArthur J (1997). Prospects for therapy of HIV-associated neurologic diseases. *J NeuroVirol* **3:** 89–101.

Sharer LR (1992). Pathology of HIV-1 infection of the central nervous system. A review. *J Neuropathol Exp Neurol* **51:** 3–11.

Suarez S, Baril L, Stankoff B, Khellaf M, Dubois B, Lubetzki C, Bricaire F, Hauw JJ (2001). Outcome of patients with HIV-1-related cognitive impairment on highly active antiretroviral therapy. *AIDS* **15:** 195–200.

Weed MR, Gold LH (2001). Paradigms for behavioral assessment of viral pathogenesis. *Adv Virus Res* **56:** 583–626.

Wit FW, van Leeuwen R, Weverling GJ, Jurriaans S, Nauta K, Steingrover R, Schuijtemaker J, Eyssen X, Fortuin D, Weeda M, de Wolf F, Reiss P, Danner SA, Lange JM (1999). Outcome and predictors of failure of highly active antiretroviral therapy: one-year follow-up of a cohort of human immunodeficiency virus type 1-infected persons. *J Infect Dis* **179:** 790–798.

Zink MC, Amedee AM, Mankowski JL, Craig L, Didier P, Carter DL, Munoz A, Murphey-Corb M, Clements JE (1997). Pathogenesis of SIV encephalitis. Selection and replication of neurovirulent SIV. *Am J Pathol* **151:** 793–803.

Zink MC, Coleman GD, Mankowski JL, Adams RJ, Tarwater PM, Fox K, Clements JE (2001a). Increased macrophage chemoattractant protein-1 in cerebrospinal fluid precedes and predicts simian immunodeficiency virus encephalitis. *J Infect Dis* **184:** 1015–1021.

Zink MC, Coleman GD, Mankowski JL, Adams RJ, Tarwater PM, Fox K, Clements JE (2001b). Increased macrophage chemoattractant protein-1 in cerebrospinal fluid precedes and predicts simian immunodeficiency virus encephalitis. *J Infect Dis* **184:** 1015–1021.

Zink MC, Spelman JP, Robinson RB, Clements JE (1998). SIV infection of macaques—modeling the progression to AIDS dementia. *J NeuroVirol* **4:** 249–259.

Zink MC, Suryanarayana K, Mankowski JL, Shen A, Piatak M Jr, Spelman JP, Carter DL, Adams RJ, Lifson JD, Clements JE (1999). High viral load in the cerebrospinal fluid and brain correlates with severity of simian immunodeficiency virus encephalitis. *J Virol* **73:** 10480–10488.